Biochimica et Biophysica Acta 1797 (2010) 1343–1352

Contents lists available at ScienceDirect

Biochimica et Biophysica Acta

journal homepage: www.elsevier.com/locate/bbabio

Review

# The mechanism of rotating proton pumping ATPases

Mayumi Nakanishi-Matsui [a,*], Mizuki Sekiya [a], Robert K. Nakamoto [b], Masamitsu Futai [a]

[a] Department of Biochemistry, Faculty of Pharmaceutical Sciences, Iwate Medical University, Yahaba, Iwate 028-3694, Japan
[b] Department of Molecular Physiology and Biological Physics, University of Virginia, Charlottesville, VA 22908-0886, USA

ARTICLE INFO

*Article history:*
Received 6 October 2009
Received in revised form 8 February 2010
Accepted 11 February 2010
Available online 17 February 2010

*Keywords:*
ATP synthase
F-ATPase
V-ATPase
Subunit rotation
Single molecule observation
Thermodynamic analysis

ABSTRACT

Two proton pumps, the F-ATPase (ATP synthase, $F_oF_1$) and the V-ATPase (endomembrane proton pump), have different physiological functions, but are similar in subunit structure and mechanism. They are composed of a membrane extrinsic ($F_1$ or $V_1$) and a membrane intrinsic ($F_o$ or $V_o$) sector, and couple catalysis of ATP synthesis or hydrolysis to proton transport by a rotational mechanism. The mechanism of rotation has been extensively studied by kinetic, thermodynamic and physiological approaches. Techniques for observing subunit rotation have been developed. Observations of micron-length actin filaments, or polystyrene or gold beads attached to rotor subunits have been highly informative of the rotational behavior of ATP hydrolysis-driven rotation. Single molecule FRET experiments between fluorescent probes attached to rotor and stator subunits have been used effectively in monitoring proton motive force-driven rotation in the ATP synthesis reaction. By using small gold beads with diameters of 40–60 nm, the *E. coli* $F_1$ sector was found to rotate at surprisingly high speeds (>400 rps). This experimental system was used to assess the kinetics and thermodynamics of mutant enzymes. The results revealed that the enzymatic reaction steps and the timing of the domain interactions among the β subunits, or between the β and γ subunits, are coordinated in a manner that lowers the activation energy for all steps and avoids deep energy wells through the rotationally-coupled steady-state reaction. In this review, we focus on the mechanism of steady-state $F_1$-ATPase rotation, which maximizes the coupling efficiency between catalysis and rotation.



## 1. Introduction

Two proton pumping ATPases, the F- and V-ATPases, are structurally and mechanistically similar, but have different physiological roles (for reviews, see [1–11]). They are entirely different from the gastric and yeast plasma membrane proton pumping P-type ATPases (P-ATPases), which form an aspartyl–phosphate intermediate during the course of the reaction cycle [6,12,13]. The F-ATPase is a ubiquitous well conserved complex found in mitochondria, chloroplasts, and bacterial membranes, and plays a central role in energy transduction [6]. This enzyme synthesizes ATP coupled to the electrochemical proton gradient formed by electron transfer chains. In contrast, the V-ATPase located on endomembrane organelles or plasma membrane is involved in acidification of organellar lumens or extracellular compartments [4,9]. A characteristic feature of the V-ATPase is its subunit diversity: six subunits have two to four isoforms specific for different organelles or cell types [7,9,10]. The presence of a specific V-ATPase is important for organellar function as well as targeting of this enzyme to a proper destination.

Despite their different physiological roles, the F- and V-ATPases are similar in subunit structure and mechanism [3,6,7,9,10]. They are reversible ATP hydrolases/synthases coupled to proton transport. In some situations, V-ATPases synthesize ATP when an electrochemical proton gradient is applied [14,15]. In both enzymes, the three catalytic sites are not independent. The steady-state ATP synthesis and hydrolysis reactions are highly cooperative mechanisms and involve all three catalytic sites in each β subunit. Boyer proposed the basic catalytic scheme, called the binding change mechanism, which predicted that the F-ATPase utilizes a rotational mechanism [16] (the body of biochemical evidence supporting rotational catalysis is summarized in [1]). The physical features of the bovine $F_1$ discovered in the first X-ray structure clearly showed that a rotation mechanism was feasible [17]. Quickly, investigators produced indirect biochemical evidence for the rotation of the γ subunit: polarized adsorption relaxation after photobleaching of eosin attached to the carboxyl terminus of the γ subunit showed ATP-dependent changes in orientation [18]; ATP hydrolysis-dependent changes of chemical cross-linking between the β and γ subunits [19]; and images captured by cryo-electron microscopy showed positional changes of subunits [20]. Finally, rotation was directly observed by attaching a fluorescently-tagged actin filament to the γ subunit of the *Bacillus* PS3 $F_1$ enzyme complex and watching the actin filament rotate in an ATP hydrolysis-dependent manner relative to the rest of the $F_1$ complex [21]. Rotation of the entire rotor group, $\varepsilon\gamma c_{10}$, relative to the complete F-ATPase

*Abbreviations:* F-ATPase, ATP synthase; V-ATPase, vacuolar-type ATPase; FRET, fluorescence resonance energy transfer; rps, revolution per second

* Corresponding author. Nishitokuta 2-1-1, Yahaba, Shiwa, Iwate 028-3694, Japan. Tel./fax: +81 19 698 1843.
*E-mail address:* nakanim@iwate-med.ac.jp (M. Nakanishi-Matsui).

0005-2728/$ – see front matter © 2010 Elsevier B.V. All rights reserved.
doi:10.1016/j.bbabio.2010.02.014

complex was demonstrated by observations of actin probes attached to each of the subunits [22–25]. Since the initial single molecule observation, the rotational mechanism of F-ATPase has been extensively studied using improved techniques as will be described in this review.

In this article, we concentrate on the rotational catalytic mechanism revealed by single molecule experiments using probes causing little to no viscous drag. Unfortunately, due to space limitations, we are unable to discuss several important findings directly related to our main topic, but refer the reader to several excellent recent reviews [11,26,27].

## 2. The ATPase structures are designed for rotation

### 2.1. Catalytic sector and stalks

The F-ATPases and V-ATPases have some common structural features that investigators have found to be important for a rotational mechanism. The basic subunit structure of F-ATPase including that of *E. coli* is $\alpha_3\beta_3\gamma\delta\varepsilon ab_2c_{10}$, and that of yeast V-ATPase is $A_3B_3CDE_2FG_2Hac_4c'c''d$ (no *c*' has been found in mammals). Both the membrane extrinsic catalytic sectors ($F_1$ and $V_1$), and the membranous proton translocation sectors ($F_o$ and $V_o$) have rotational mechanisms [3,6,7,9–11] (Fig. 1). The nucleotide binding subunits ($\alpha_3\beta_3$ in $F_1$ or $A_3B_3$ in $V_1$) and the proton translocation subunits in the membrane ($ac_{10}$ or $ac_4c'c''$) are connected by the central (γε or DF*d*) and peripheral ($\delta b_2$ or $CE_2G_2Ha$) stalks. The $F_1$ rotor subunit γ is located at the center of the $\alpha_3\beta_3$ pseudo-hexamer [17] and together, $\alpha_3\beta_3\gamma$, defines the minimal complex required for rotational catalysis. γ and ε subunits directly connect to the proton translocating *c* subunit ring [28].

Mutagenesis studies helped to identify the F-ATPase amino acids that are involved in catalysis [6,29–33]. βLys155 and βArg182 in the β subunit were shown to be required for binding of the γ-phosphate moiety of ATP [34–38], while the hydroxyl moiety of βThr156 is essential for $Mg^{2+}$ binding [35,39]. βGlu181 is a critical catalytic residue which forms a hydrogen bond with a water molecule located near the ATP γ-phosphate [17,36]. The βGlu185 residue may be involved in promotion of catalysis to steady-state turnover [40]. All these residues are conserved in the V-ATPase, suggesting that it has the same catalytic mechanism as the F-ATPase [6]. Similarly, genetic, biochemical, kinetic and thermodynamic analyses were used to identify the roles of γ subunit residues in catalysis and energy coupling [6,41–46].

On the other hand, there are distinct structural differences between the F- and V-ATPases. The subunit composition of the peripheral stalk of V-ATPase is more complex than that of F-ATPase because the V-ATPase C, E, G, H, and *a* subunits have two to four isoforms each [7]. These subunits may be related to the reversible disassembly/reassembly regulatory mechanism specific to the V-ATPase [9].

### 2.2. Proton-transporting sector

In the F-ATPase, ATP hydrolysis in the β subunits couples to rotation of the $\gamma\varepsilon c_{10}$ complex against the stator ($\alpha_3\beta_3\delta ab_2$), which drives uphill proton transport. The mechanism of proton translocation occurs at the interface between *a* and *c* subunits and specifically involves proton binding residues *a*Arg210 and the Asp61 of the rotating *c* ring [5,47–49]. In the reverse or physiological condition, the electrochemical gradient of protons drives rotation of the *c* ring, which couples to ATP synthesis in $F_1$. The number of *c* subunits in a complex appears to be dependent on the source. The ATP synthases of yeast mitochondria, *E. coli*, and *Bacillus* PS3 have 10 subunits in their *c* rings [50–52]. In contrast, those of *Ilyobacter tartaricus* and *Propionigenium modestum* have 11 *c* subunits [53,54], while that of chloroplasts has 14 subunits [55,56], and cyanobacterium *Spirulina platensis* contains 15 *c* subunits [57]. Assuming one proton per *c* subunit, the number of *c* subunits in the ring complex implies the number of protons transported during the course of a 360° rotation, 10–15 protons in the above mentioned examples, or 3.3–5 protons per ATP synthesized or hydrolyzed. The proton/ATP coupling ratio of ATP synthases are probably optimized for their specific physiological condition.

The similar subunit structure of the V-ATPase suggests the $DFc_4c'c''$ complex along with perhaps the *d* subunit acts as the rotor [9]. Because a single proton-transporting Glu residue is found in each of the *c*, *c*' and *c*" subunits which form the transmembrane rotor ring, rotation of the $c_4c'c''$ ring likely translocates only six protons per 360° rotation. Therefore, two protons are pumped per ATP hydrolyzed implying that the V-ATPase requires a much higher proton motive force to drive the reverse ATP synthesis direction [58].

The direction of the chemical reaction (ATP hydrolysis or synthesis), which is directly coupled to the direction of proton transport, and therefore the direction of subunit rotation, appears to

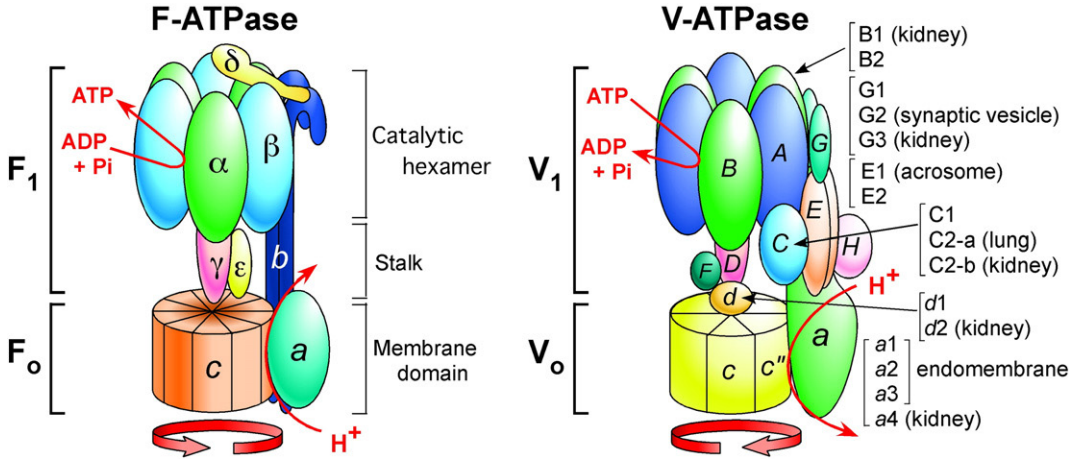


**Fig. 1.** Schematic models of the F-ATPase (*E. coli*) and V-ATPase (mammalian). The membrane extrinsic ($F_1$ and $V_1$) sectors, catalytic hexamers ($\alpha_3\beta_3$ and $A_3B_3$, respectively), stalks, and membrane domains ($F_O$ and $V_O$) are shown. Red arrows represent the direction of the chemical reaction, subunit rotation, and proton transport in physiological conditions. Diverse isoforms of V-ATPase are shown with their specific localization [7,9]. Those not indicated are ubiquitous.

be regulated by the energy state of the cell. The energetic balance of the ATP/ADP concentration ratio and the electrochemical proton gradient exclusively define whether the enzyme operates as an ATP synthase or an ATPase [6,7]. Similar to the reversibility of the F-type ATP synthase to hydrolyze ATP, the V-ATPase synthesizes ATP in some cases [14,15]. Finally, we note that the basic structure of V-ATPase is very similar and mechanically the same as that of the F-ATPase. Common structural features of these ATPases are exquisitely designed for coupling the rotational catalytic and proton transport mechanisms.

An interesting question is which sector of ATPase rotates physiologically because the rotor or stator has been defined by *in vitro* single molecule studies. In this regard, Holliday et al. and Lu et al. found that the B and E subunits of V-ATPase bind actin and aldolase, respectively [59,60]. The interaction with actin likely immobilizes the $A_3B_3$ hexamer, and thereby causes the $A_3B_3$ hexamer to act as a stator. A similar protein interaction is unknown for F-ATPase.

## 3. Rotational catalysis in the F-ATPase

### 3.1. Observation of subunit rotation

In 1979, Paul Boyer [16] suggested that the F-ATPase catalytic mechanism involved rotation of an $F_1$ subunit relative to the three catalytic sites. The crystal structure of the $\alpha_3\beta_3\gamma$ complex reported in 1994 by Walker and colleagues [17] rekindled this idea. Several investigators set out to design experiments that would prove such a mechanism. Indirect biochemical approaches led to results that were consistent with ATP-dependent γ subunit rotation (described above). Finally, rotation was conclusively shown by direct observation in single molecule experiments. Noji et al. reported the ATP-dependent rotation of a fluorescently-labeled actin filament attached to the γ subunit of *Bacillus* PS3 $F_1$ [21]. Using similar methods, rotation of the *E. coli* γ subunit was also shown to rotate indicating that rotation was a general mechanism of the $F_1$ enzyme [61].

Subsequently, rotation in the $F_o$ transport sector was shown by fixing the detergent-solubilized $F_oF_1$ complex on a glass surface via the α subunit with a fluorescent probe attached to the rotor *c* subunit ring [23], or the $F_oF_1$ fixed to the surface via the *c* ring with the probe attached to the β subunits [24,62]. The results demonstrate that the rotor and stator are interchangeable. Rotation of membrane-bound $F_oF_1$ has also been shown experimentally [25], establishing that the *c* ring rotates relative to the *a* and β subunits. Rates of ATP-driven γ subunit rotation in $F_1$ and ATP-driven $\gamma\varepsilon c_{10}$ rotation in $F_oF_1$ are very similar in the two complexes with a calculated frictional torque of ~40 pN nm. The rotation of $\gamma\varepsilon c_{10}$ was consistent with results of inter-subunit cross-linking experiments [63,64] where a disulfide bond between γ and *c* subunits had little or no effect on ATP hydrolysis or synthesis, while cross-links between γ and β, or γ and α, resulted in loss of steady-state ATPase activity. In this regard, Scanlon et al. [65] showed by pre-steady-state analysis that γ–β cross-linked enzyme can hydrolyze the first ATP but not other bound ATP. Other single molecule FRET experiments also observed that the γ and ε subunits rotate relative to the *b* subunits in membrane-bound $F_oF_1$ [66,67].

While ATP hydrolysis-dependent rotation of $\gamma\varepsilon c_{10}$ is always observed in one direction, one expects that ATP synthesis driven by proton flow through the $F_o$ should rotate in the reverse direction. This hypothesis was proven by showing rotation in the expected direction during ATP synthesis in $F_oF_1$ reconstituted in liposomes. In this case, FRET was used to report the real time changes in distances between probes attached to *b* and γ subunits, or ε and *b* subunits [66–68]. As predicted, the direction of rotation during ATP synthesis was reversed to that of ATP hydrolysis. Similarly, artificially forced rotation of γ in the same direction was shown to drive ATP synthesis. Itoh et al. [69] and Rondelez et al. [70] observed a low but significant level of ATP synthesis when a bead firmly attached to γ was forced to rotate. These results established beyond the shadow of any doubt the mechano-chemical coupling between ATP synthesis/hydrolysis and the electrochemical gradient of protons.

### 3.2. Mechanical rotation and ATPase reaction

#### 3.2.1. Can rotation of the γ subunit be resolved into steps that are related to the chemical reaction kinetics?

The binding change mechanism indirectly predicts that a rotary mechanism is intimately involved in the mechanism of ATP synthesis and hydrolysis [16]. Using the thermophilic *Bacillus* PS3 $F_1$ at ATP concentrations well below the $K_m$, γ subunit rotation was found to dwell in distinct 120° steps [71,72] (Fig. 2). Because the duration of the pause depends upon the ATP concentration, the pause was attributed to the enzyme waiting for an ATP binding event (ATP-waiting dwell) (Fig. 2, blue line). Experimental set-ups with better time resolution using 40-nm diameter gold beads revealed that the 120° steps were divided into 80° and 40° substeps [73]. The duration of the pause before the 80° substep became shorter with increasing ATP concentration, once again suggesting the ATP-waiting dwell (Fig. 2, blue line). In contrast, the pause duration before the 40° substep was significantly increased by the slow hydrolysis rate when ATPγS was used as a substrate, or by the catalytic site mutation βE190D (*Bacillus* numbering) [74]. Together these data indicate that the pause duration before the 40° substep is the catalytic dwell (Fig. 2, red line), or the time during reversible ATP–ADP hydrolysis/synthesis step [75].

#### 3.2.2. Does ATP bind to all catalytic sites at the same time?

Nadanaciva et al. suggested that two out of three catalytic sites have the capability of forming a transition state between ATP and ADP + Pi simultaneously. Their hypothesis was based on the observation that two sites were titrated with fluoroscandium (ScFx) plus ADP, the complex of which, $F_1$-ADP–ScFx, mimics a catalytic transition state [76]. Consistent with this result, analysis of the $F_1$ crystal structure found that the three catalytic sites were occupied by ATP, ADP, or devoid of nucleotide, and thus the corresponding conformations were designated $\beta_{TP}$, $\beta_{DP}$, and $\beta_E$, respectively [17] (Fig. 3). Simultaneous observation of rotation and Cy3–ATP bound to the catalytic site suggested that one ATP (ADP) molecule remained bound to a catalytic site for at least 240° of γ subunit rotation. This ATP appeared not hydrolyzed upon binding but rather hydrolyzed after the first 120° revolution [77]. These results indicated that the reactions at the three catalytic sites were not simultaneous but rather occurred sequentially in a highly cooperative fashion: for each 120° step, ATP binds to one β subunit, ADP is released from the second β subunit, ATP is hydrolyzed in the third β subunit, and Pi is released from the second β [78,79].

In contrast, a different kinetic pathway was proposed based on pre-steady-state kinetic analysis using millisecond mixing experiments. Scanlon et al. proposed a model where ATP binds to one β subunit after ADP release, ATP in the second β is hydrolyzed, and Pi and ADP in the third β are released within one 120° step [75]. In this model, all three catalytic sites should bind nucleotides transiently, as shown in the kinetic scheme in Fig. 2. Consistent with this model, crystals grown in the presence of ADP and aluminum fluoride showed the $F_1$ enzyme in a conformation with nucleotides bound to all three β subunits [80].

#### 3.2.3. Does Bacillus PS3 $F_1$ exhibit the same rotational scheme at its physiological temperature?

All experiments on the thermophilic *Bacillus* were carried out below ~24 °C, whereas the organism optimally grows at 75 °C. Thus far, few single molecule experiments have addressed this question, although $F_1$ was recently studied at 4–50 °C [81]. In this regard, the advantage of studying the mesophilic enzyme from *E. coli* should be noted because it is easily studied in its physiological temperature range between 25 and 37 °C.

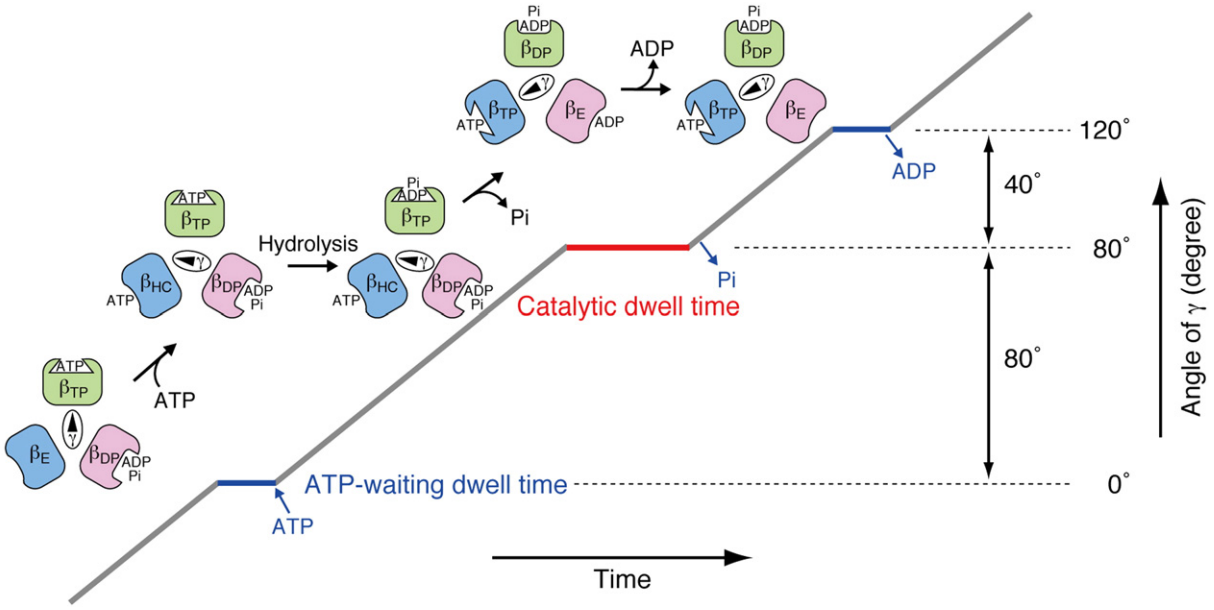


**Fig. 2.** Scheme of $F_1$ rotational catalysis. A model of the relationship of the chemical reaction to the β subunit conformation, and the position of the γ subunit at ATP concentrations below the $K_m$ are shown. The ATP-waiting dwell time is the time waiting for ATP binding (blue line). The catalytic dwell time is the time for ATP hydrolysis and Pi release (red line). Note that the γ-β subunit interactions are different for each β subunit. $\beta_{TP}$, $\beta_{DP}$, $\beta_E$, and $\beta_{HC}$ are the β subunits with ATP or ADP bound, empty, or half closed, respectively. Modified from Sekiya et al. [86].

## 4. Toward understanding the rotation mechanism

### *4.1. Subunit rotation and steady-state ATPase*

Discussion in this section is focused mainly on the *E. coli* F-ATPase. Extensive genetic and biochemical analyses provide many tools for dissecting the mechanism of catalysis coupled to transport [6]. Similar to the case of the thermophilic enzyme, the rotation speed of an actin filament attached to the γ subunit was ~10 rps, which was much slower than the 30 rps expected based on steady-state ATPase rates [61]. Obviously, the high viscous drag generated by actin (~1–2 μm in length) would decrease the speed. In addition, the long length of the filament also caused relatively large deviations in the data, which made kinetic analyses difficult to interpret.

These considerations prompted us to use small gold beads as probes for observation of subunit rotation, which allowed the enzyme

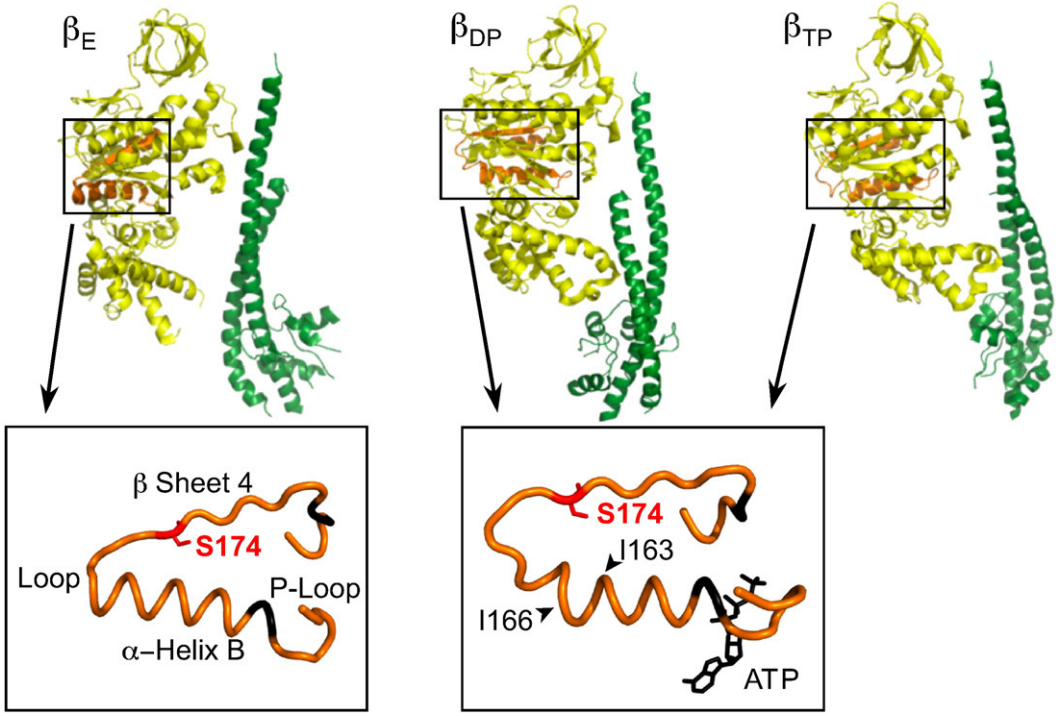


**Fig. 3.** The structures of the bovine β and γ subunits (PDB ID: 2JDI) [99]. Yellow and green represent the β and γ subunits, respectively. The catalytic β subunits adopt different conformations with different nucleotide occupancies. The expanded figure (orange) shows the β subunit hinge domain (P-Loop/α-HelixB/Loop/β-Sheet4, βPhe148–βGly186) including the catalytic residues (βLys155, βThr156, βGlu181, and βArg182, in black with *E. coli* numbering). The conformation of this domain changes dramatically upon nucleotide binding.

to operate unencumbered [82] (Fig. 4a). The rotation rate was dependent on the bead size, but was generally much faster than that achievable with the actin filaments. Significantly, we found that 40 and 60 nm diameter beads rotated at very similar rates, 455 ± 79 and 427 ± 66 rps, whereas those of 80, 100, and 200 nm beads were 320 ± 38, 266 ± 29, and 110 ± 21 rps, respectively [82] (Fig. 4b). These results indicated that 40 and 60 nm beads were small enough to rotate without imparting drag, and thus provided the ability to analyze the rotational behavior with minimal artifacts of the experimental system.

We also note that we decided to calculate rotation rates from full 0.25 s data sets regardless of the length of pauses, rather than only using data from beads that were observed to rotate continuously. Interestingly, we found that the observed rotation rate of 381 ± 33 rps from 0.25 s data sets that included long pauses was ~10 times faster than the value estimated from the bulk steady-state ATPase activity, which was ~30 rps, assuming that 3 ATP were hydrolyzed per revolution [82]. We concluded that the discrepancy was because ~90% of the $F_1$ molecules were inactive or in an inhibited state at any given point during our standard 0.25 s rotation observations. We observed much longer pauses of rotation than the catalytic dwell times (~1 ms) even when assayed for 0.25 s [82]. As can be surmised from the numbers of pauses, the extended observation time of 2 s typically contained pause durations of longer than 1 s [83] (Fig. 4c), which would not be detected in shorter observation windows. These long pauses were likely due to Mg·ADP inhibition or the inherent behavior of the rotary enzyme [83]. These long pauses were possibly part of the mechanism regulating ATP hydrolysis by F-ATPase. Significantly, bulk phase steady-state ATPase activity was approximated by the combination of the averaged rotation rate and the time of long pauses over many observations. Therefore, long pauses appeared to be an important component of the ensemble steady-state ATPase activity. The reason for the difference between the observed rotation rate and the ATPase activity could be because all long pauses were not included in 0.25 s observations [82]. As shown in Fig. 4c, even the 2 s observation was sometimes not enough for quantitative analysis of long pauses because some pauses lasted longer (e.g. *red* and *gray* time courses). However, when rotation was observed for 16 s, almost all long pauses could be included and the overall average rotation rate (rate estimated from rotation and long pauses) was consistent with the bulk ATPase activity (M. Sekiya, H. Hosokawa, M. Nakanishi-Matsui, and M. Futai, in preparation).

### 4.2. Stochastic fluctuation and effect of the ε subunit

Single molecule observation is a powerful method for following the continuous reaction of individual molecules. When time courses are expanded, at least in the case of the *E. coli* $F_1$, rotation speeds vary to a significant degree. Histograms of rates at 10 ms intervals show the expected stochastic fluctuation of rotation rates [82,84,85]. To further evaluate the fluctuation, single revolution times, i.e., the time length required for single 360° revolutions, were estimated [83]. This

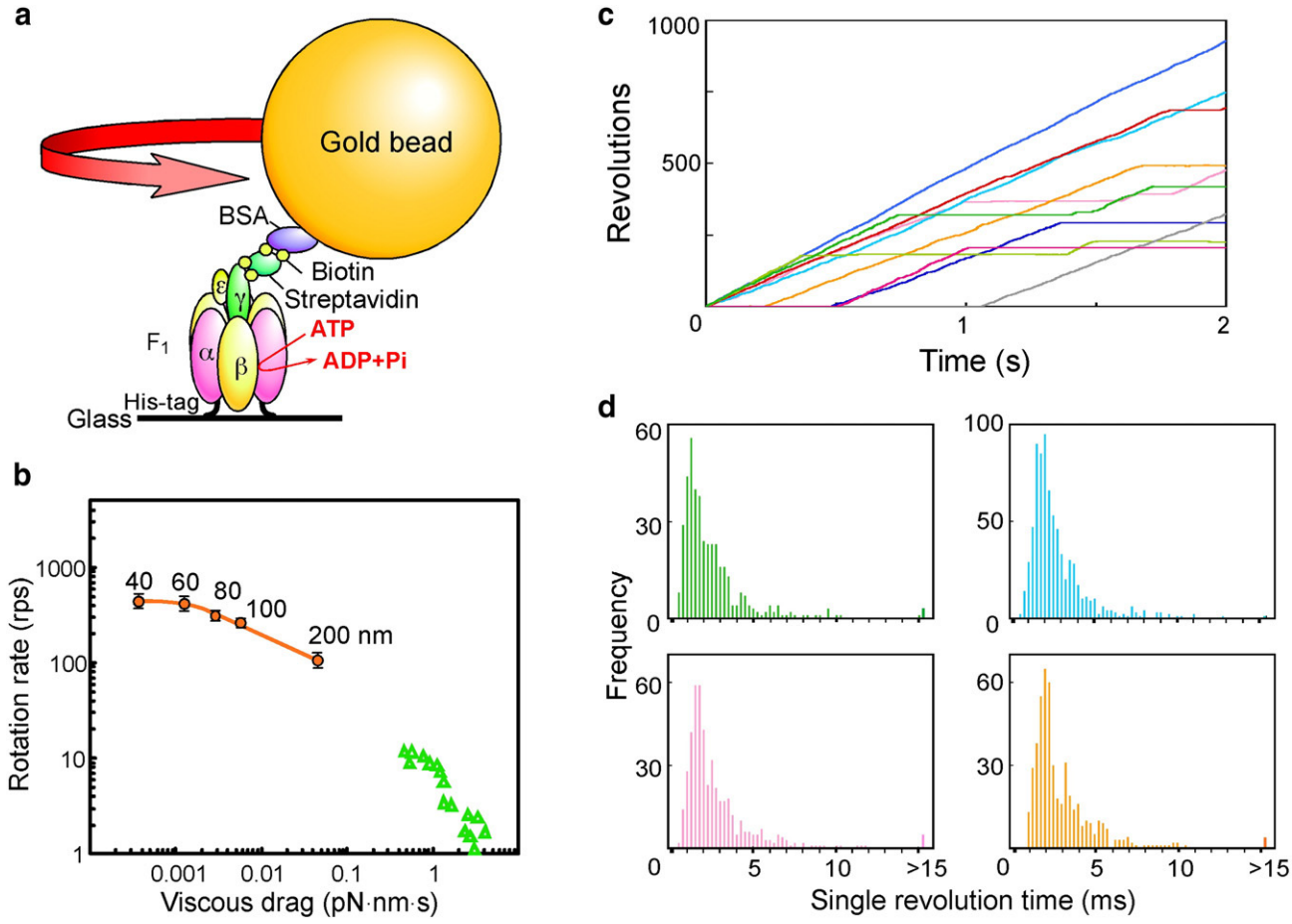


**Fig. 4.** Single molecule observation of $F_1$ subunit rotation. (a) The experimental setup for observing gold bead rotation. $F_1$ was immobilized on a glass surface and a bead attached to the γ subunit through streptavidin and BSA (bovine serum albumin). The laser light reflected from the gold bead was observed under a dark field microscope and recorded by a charge coupled device camera. (b) Average rotation rates for various sized gold beads (orange circles) and actin filaments (green triangles). Average rotation rates were plotted against the corresponding viscous drag. (c) Time courses of 60 nm gold beads followed for 2 s in the presence of 2 mM ATP. Different colors represent the rotation of 10 individual gold beads. (d) Examples of histograms of single revolution times obtained for single beads ($n = 4$) are shown. The colors correspond to those in (c).
Cited and modified from Nakanishi-Matsui et al. [82,83].

analysis included all rotations regardless of the duration of the pauses. Summarized histograms for individual beads clearly showed similar fluctuations (Fig. 4d) indicating that the fluctuation is an intrinsic property of this enzyme.

Although the effect of the ε subunit, an inhibitor of $F_1$-ATPase activity, on rotation has not been observed using actin filaments, the average rate of 60 nm beads was clearly inhibited about 50% upon the addition of super-stoichiometric concentrations of ε subunit [82,85]. Although long pauses were rarely observed in 0.25 s observations, pauses longer than 50 ms were sometimes observed in the presence of excess ε [82]. These results suggest that ε subunit inhibits rotation by decreasing the rotation rate and by increasing the frequency of long pauses. To analyze the ε effect on long pauses quantitatively, longer observations are necessary.

### 4.3. Rate determining step of rotation through a flat energy pathway

Each catalytic site should assume at least four states during ATP hydrolysis: ATP binding, ATP hydrolysis, ADP release, and Pi release. As Abrahams et al. discovered in the high resolution X-ray structure, a critical feature of $F_1$-ATPase is the inherent asymmetry of the three β subunits in different conformations, $\beta_{TP}$, $\beta_{DP}$, and $\beta_E$, the conformations of which correspond to the nucleotide bound in each catalytic site, ATP, ADP and empty, respectively [17]. During the course of steady-state rotational catalysis, one catalytic site binds ATP, while a different site carries out hydrolysis, and the third site releases Pi [6,45,73,78,79]. The conformation of the given β subunit is conferred by the side of the asymmetric γ subunit it faces, as shown in Fig. 3.

The next question is how the steady-state catalytic reaction steps are coordinated to the rotation of the $\gamma\varepsilon c_{10}$ complex and therefore the conformations of the three β subunits. Pre-steady-state analysis of the burst kinetics of ATP hydrolysis in nearly $V_{max}$ conditions demonstrated that the rate-limiting transition state occurs after the reversible hydrolysis/synthesis step and before the release of Pi [65,75]. The kinetics of steady-state hydrolysis can only be assessed when the ATP concentration is high enough to fill all three catalytic sites. In such conditions, $F_1$-ATPase exhibits continuous 120° steps, consisting of short pauses (<1 ms) (Fig. 5a, red line) and 120° rotation steps (Fig. 5a, gray line) [83]. Because the ATP-waiting dwell times are too short to be detected with millisecond time resolution, the observed duration of the short pauses should be the catalytic dwell times, or the times required for ATP hydrolysis. Significantly, the duration of the catalytic dwell became slightly shorter with increasing temperature; the average dwell times at 17 and 31 °C were $0.22 \pm 0.014$ ms and $0.15 \pm 0.016$ ms, respectively [86]. The time for the 120° rotation was longer than the pause duration and also became shorter with temperature: $0.84 \pm 0.055$ ms at 17 °C and $0.53 \pm 0.037$ ms at 31 °C. The reciprocal of the 120° rotation time was used to calculate the speed of the 120° rotation, which increased with temperature: $1206 \pm 80\ s^{-1}$ at 17 °C and $1917 \pm 127\ s^{-1}$ at 31 °C. Arrhenius slopes of the speed of the individual 120° revolution steps (open circles) and the reciprocal of the average pause duration (closed circles) were *linear and very close in value* (Fig. 5b), indicating that they had similar activation energies, $E_A$, and thus similar rate constants for the revolution and pause steps between 17 and 31 °C [86]. These results indicate that there is no distinct rate-limiting transition state in the steady-state reaction cycle. Thus, the energy pathway is relatively flat, and the enzyme avoids distinct energy peaks and valleys. Clearly, the highly cooperative, three site motor is exquisitely designed to operate in a smooth rotational cycle.

### 4.4. Generation of driving force in the β subunit

The crystal structure of bovine $F_1$ revealed that the three catalytic β subunits adopted distinct conformations with different nucleotide occupancies. The β subunit hinge domain [P-loop (phosphate-binding loop)/α-helix B/loop/β-sheet 4, βPhe148–βGly186] including the catalytic residues (βLys155, βThr156, βGlu181, βArg182, and βGlu185, *E. coli* numbering) [6] dramatically changed its conformation upon nucleotide binding (Fig. 3) [17]. The conformational change in the hinge domain is transmitted to the β subunit $^{380}$DELSEED$^{386}$motif, which pushes the γ subunit to rotate. This hypothesis has been supported by recent NMR analysis of the β monomer with nucleotide bound [87]. We investigated the rotation of mutant $F_1$ complexes with an amino acid replacement in the (1) hinge domain and (2) at the interface between γ and the $\beta^{380}$DELSEED$^{386}$ motif.

The $F_1$ mutant with the Ser174 in β-sheet 4 replaced by Phe (βS174F) (Fig. 3) has been extensively characterized and has about 10% of the wild type ATPase activity [88]. Consistent with the low activity, the rotation speed of this mutant was clearly slower than that of the wild type [83,85]. Similar to the wild type, the mutant exhibited three 120° steps per revolution in $V_{max}$ conditions. Most importantly, the mutant catalytic dwell times were about 10 times longer than those of the wild type [83]. Thus, the slower rate of the ATP hydrolysis and product release steps decreased the overall mutant rotation rate. The Phe replacement of the native Ser possibly stabilized the hinge domain when the nucleotide binding site was occupied.

Based on the crystal structure of the bovine enzyme, homology modeling of the *E. coli* β subunit predicted a hydrophobic interaction between βIle163 and the Phe introduced at position β174. The calculated energy of interaction is −0.47 kcal/mol [89], which is low but not insignificant. We hypothesized that the additional interaction caused a large effect on rotation because no other strong interaction was predicted in the hinge domain. Further modeling suggested that the replacement βI163A would reduce the interaction between βIle163 and βS174F, whereas βI166A would not affect the interaction (Fig. 3). As expected, βI163A resulted in increased rotation rates of the βS174F mutant, but βI166A was without effect [89]. These results suggest that the interaction between βIle163 and βS174F stabilizes the hinge domain in the nucleotide bound form. This stabilization probably inhibits the smooth conformational change of the hinge domain, which is necessary for driving high-speed rotation.

### 4.5. A pertinent interaction between the β and γ subunits

An active role of the γ subunit in the F-ATPase has been suggested by the behavior of a series of mutants with low ATPase activity or defective energy coupling between catalysis and proton transport [41,42,90]. Among them, the most interesting is replacement of γMet23 with a positively charged amino acid. Alignment of the known γ subunit sequences reveals that conserved residues are clustered in the amino- and carboxyl terminal regions, and γMet23 is one of the few completely conserved residues [42]. Replacement of γMet23 by Arg or Lys perturbed the coupling between ATPase activity and proton transport [42]. The uncoupling is probably due to an altered β–γ interaction because all second site suppressor mutations are located in the β–γ interface [43,44]. As one would surmise from the rotation of the γ subunit and its influence on the β subunit conformations, the β–γ interactions must play specific roles in the transmission of conformational information to the β subunits. Although most of the second site mutations were distant from the γM23K site, the X-ray crystal structure indicated a close interaction between γMet23 and βGlu381 of the $\beta_{DP}$ $^{380}$DELSEED$^{386}$ motif [17] (Fig. 5c). We speculated that the positively charged Lys or Arg at position γ23 formed an ionized hydrogen bond with βGlu381. Consistent with this notion, replacement of βGlu381 with Ala, Asp, or Gln suppressed the uncoupling effect of γM23K [46].

Importantly, Al-Shawi and Nakamoto [91] and Al-Shawi et al. [45,92] found that the γM23K mutation strongly affected the rate-limiting transition state of steady-state ATP hydrolysis and ATP synthesis. To identify the rate-limiting transition state step in the

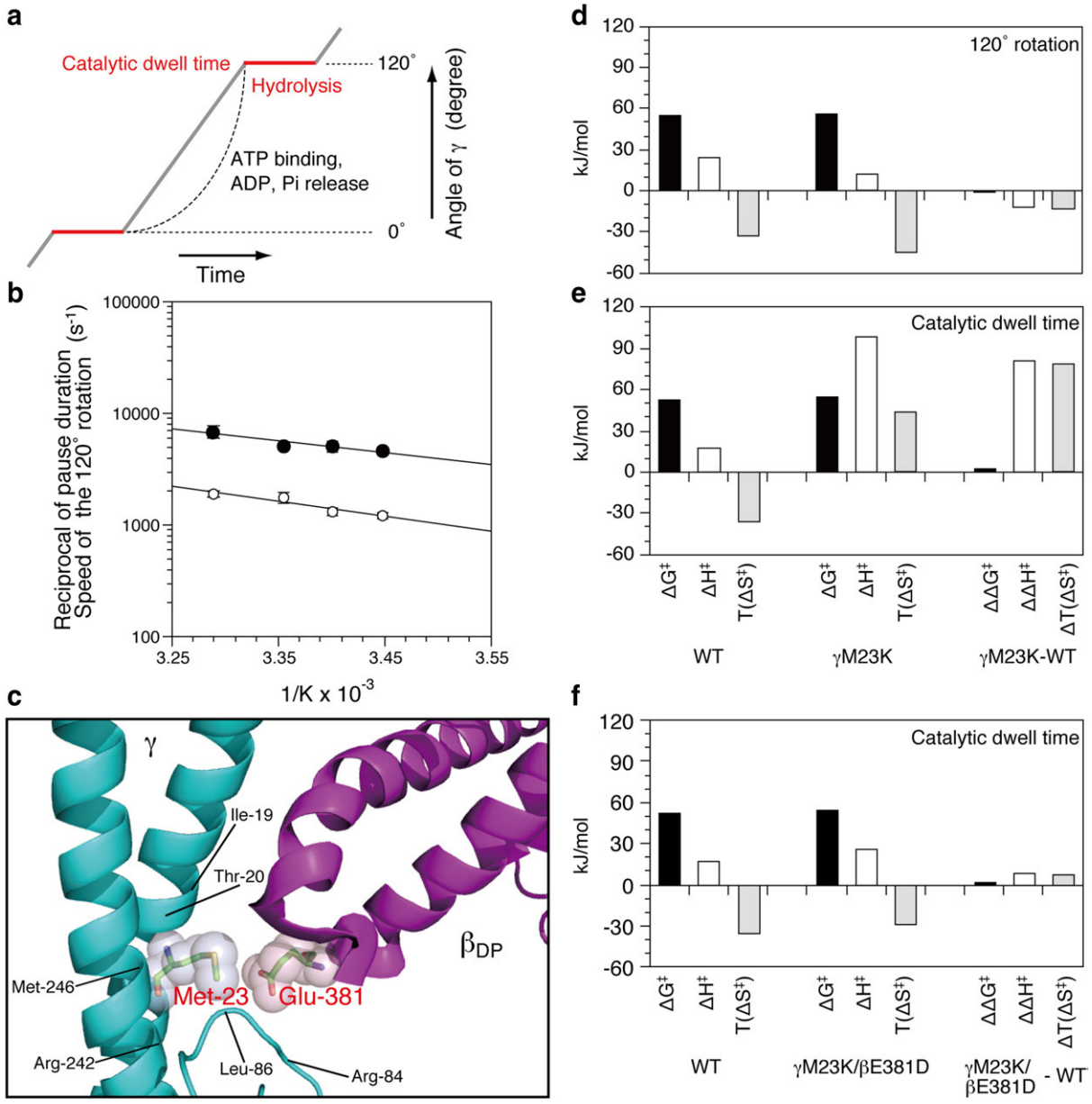


**Fig. 5.** Thermodynamic analysis of $F_1$ rotation. (a) Scheme of $F_1$ rotational catalysis in $V_{max}$ conditions. The 120° step (the catalytic dwell time (red) and 120° rotation (gray)) is shown. See also the scheme in Fig. 2 (the limiting ATP condition). (b) Arrhenius plots of the speed of the 120° rotation ($s^{-1}$) (open circles) and the reciprocal of the pause duration (closed circles) of wild type $F_1$. (c) The interface between the $\beta_{DP}$ (purple) and γ (blue) subunits. The β and γ subunits interact through γMet23 and βGlu381 in the $\beta^{380}$DELSEED$^{386}$ loop. (d–f) Transition state thermodynamic parameters at 31 °C for wild type and mutant $F_1$ rotation were calculated from the Arrhenius data for the speed of the 120° rotation step (d), and the reciprocal of the pause duration (e) of γM23K $F_1$ compared with wild type $F_1$, and the reciprocal of the pause duration of γM23K/βE381D $F_1$ compared with wild type $F_1$ (f). The differences in the parameters between the wild type (WT) and mutant $F_1$ enzymes are shown as ΔΔ values on the right.
Cited and modified from Sekiya et al. [86].

rotational behavior, the temperature dependence of γM23K $F_1$ rotation was examined in $V_{max}$ conditions [86]. The transition state thermodynamic parameters show the dramatic effect of the γM23K on the catalytic dwell time. Although the thermodynamic parameters for the stepping speed of the 120° rotation were very similar to wild type (Fig. 5d), $\Delta H^{\ddagger}$ and $T\Delta S^{\ddagger}$ for the catalytic dwell time were significantly increased by ~80 kJ/mol for γM23K compared to the wild type (Fig. 5e). These results clearly demonstrate that the mutant enzyme exhibits a dominant rate-limiting step during the catalytic dwell time. The prolonged dwell time is a manifestation of the much larger activation energy the enzyme faces at the beginning of each rotation step.

To verify that the γM23K mutation caused the greatly increased activation energy and the effect on the rotation behavior, the double mutant, γM23K/βE381D, was assessed in rotation experiments [86]. As expected, γM23K/βE381D exhibited bulk steady-state ATPase activity, single revolution times, and pause durations similar to those of the wild type. Significantly, the double mutant had very similar thermodynamic parameters compared with the wild type, in particular the catalytic dwell time (Fig. 5f). These results demonstrate that the specific interaction between the γ and β subunits (γMet23 and $\beta^{380}$DELSEED$^{386}$, respectively) plays a critical role in establishing the transition state structure of the enzyme and that the transition state occurs at the beginning of the rotation step.

## 5. Rotational catalysis of V-ATPase

As discussed above, the structure of the V-ATPase has the same basic elements as that of the F-ATPase, including the catalytic residues [4,6]. The structural similarities with F-ATPase suggest

catalysis by V-ATPase occurs by a rotational mechanism, although it has been studied less extensively. An actin filament attached to the G subunit of the yeast V-ATPase rotated upon ATP hydrolysis [93]. It is noteworthy that this experiment showed rotation of the peripheral stalk against the *c* ring immobilized on a glass surface. A bacterial homologue of the V-ATPase also exhibited rotation as subunit rotation of the *T. thermophilus* $V_1$ sector was observed relative to the $A_3B_3$ hexamer. In these experiments, a 560 nm bead was attached to the D or F subunit, which were considered to be the functional homologues of $F_1$ γ or ε subunits [94]. Rotation of *T. thermophilus* $V_oV_1$ fixed through the $A_3B_3$ complex was also observed using a bead attached to the $c_4c'c''$ ring [95]. In both cases, the torque generated during rotation was ~35 pN nm, slightly lower than that measured for the F-ATPase.

To determine if $V_1$ has a different rotation scheme from $F_1$, the substeps of the $V_1$ were recorded with a duplex of 209 nm beads attached to the $V_1$ D subunit [96]. Upon hydrolysis of ATPγS, the beads showed the expected 120° stepping rotation. After changing reaction buffer to one containing a low concentration of ATP, the same bead duplex showed 120° steps at the same orientation of the D subunit as that of ATPγS. This result indicated that catalysis and ATP binding occurred at the same D subunit orientation, whereas in F-ATPase, catalysis and ATP binding occurred at different orientations. As described above, catalysis occurs in the $F_1$ enzyme at the 80° position advanced from that of ATP binding. Based on these results, coupling between the mechanical rotation and chemistry in $V_1$ is likely to be different from that of $F_1$. The scheme comprising 40° and 80° substeps may not be an intrinsic property for rotational catalysis by all proton pumping ATPases. To elucidate the rotational mechanism of V-ATPase in more detail, the crystal structure of $V_1$ is needed as well as an experimental system for observing the rotation of a probe that imparts low viscous drag.

## 6. Perspectives

"Seeing is believing" is as true in bioenergetics as in any other field. The single molecule approach and direct observation of rotation provided a new method for answering questions regarding the complicated F- and V-ATPase enzymes. The fast rotation of the *E. coli* $F_1$ was unexpected (~430 rps at 24 °C) [82] because the *Bacillus* $F_1$ rotated much more slowly (~130 rps at 24 °C) [73]. The *E. coli* $F_1$ has an intrinsic mechanism for rotation at such a high speed. Studies of rotation are pertinent to understanding the mechanism, thermodynamics, and physiological roles. Initial probes used for observing rotation were actin filaments (~1 μm in length), but great progress has been made in the past decade using more sophisticated probes. Gold beads of 40–60 nm enabled us to analyze rotation without the artifact of viscous drag. High-speed stepped rotation, stochastic fluctuation of rotation rates, an inhibitory effect of the ε subunit, the profile of the energy pathway, and pertinent interactions in the β hinge domain or between β and γ have been demonstrated using such beads [82,83,86,89].

The progress of understanding the F- and V-ATPases raises further questions:

(1) The detailed mechanism of energy coupling between catalysis and proton transport through mechanical rotation remains unknown. As discussed above, the γ subunit rotates in $F_1$ through 120° steps, which is consistent with the three catalytic sites. In the $F_oF_1$, the integration of the catalytic 120° steps to the proton transport via the 10 proton-transporting subunit *c* Asp residues is not understood. The ratio of the number of protons transported to ATP synthesized or hydrolyzed appears not to be an integer quantity. Alternatively, the number of protons transported in each catalytic 120° step may vary to accommodate the non-integer $H^+$/ATP ratio: for example, three protons in two catalytic 120° steps and four in one 120° step may be transported in a complex with 10 *c* subunits. A similar mechanism may be expected for other organisms that have 11, 13, or 14 *c* subunits in the *c* ring [50,55,97]. Whatever the case, an elastic energy storage mechanism is most likely in the coupling of proton transport and catalysis through rotation.

(2) The rotation mechanism during ATP synthesis should be examined to confirm whether or not ATP synthesis is the complete reverse of ATP hydrolysis. It is challenging to assay rotation and chemistry driven by a proton gradient at the same time.

(3) The question remains whether the F-ATPase rotates through the same mechanism in physiological conditions. Although rotational catalysis has been studied extensively using the thermophilic *Bacillus* enzyme, the experiments were mostly performed at room temperature, i.e., far from the physiological condition of the bacterium. In this regard, further analysis using the *E. coli* enzyme is critical because it can be studied in its physiological temperature range. The next challenge is to develop the techniques to observe rotation *in situ*.

(4) Many questions about the V-ATPase remain to be answered. As mentioned above, some V-ATPase subunits have two to four isoforms that have organellar or tissue-specific distribution [6,7,9,10]. The different isoforms are involved in localization and in different biological roles. In this regard, the two E subunit isoforms, the acrosome-specific E1 and the ubiquitous E2, have different effects on $V_o$ and $V_1$ assembly [98]. It is not known if E1 confers differences in the rotation behavior compared to E2. Observation of the rotation behavior may be the most straightforward method for determining the effects of different isoforms. It is likely that the different behaviors will be reflected in the biological functions including determination of organellar pH. An experimental system for observing V-ATPase rotation with a low viscous drag probe is essential for answering these questions. Many interesting questions remain to be addressed and single molecule experiments on proton pumping ATPases will continue to fascinate us in the next decade.

## Acknowledgements

Our studies described in this article were supported by CREST (Core Research for Evolutional Science and Technology), JST (Japan Science and Technology Agency), and the Japanese Ministry of Education, Culture, and Science. Our studies were also supported by funds from the Terumo Life Science Foundation and the Japan Foundation for Applied Enzymology (to M. N.-M.).

## References

[1] P.D. Boyer, The ATP synthase—a splendid molecular machine, Annu. Rev. Biochem. 66 (1997) 717–749.
[2] J. Weber, A.E. Senior, Catalytic mechanism of $F_1$-ATPase, Biochim. Biophys. Acta 1319 (1997) 19–58.
[3] D. Stock, C. Gibbons, I. Arechaga, A.G. Leslie, J.E. Walker, The rotary mechanism of ATP synthase, Curr. Opin. Struct. Biol. 10 (2000) 672–679.
[4] T. Nishi, M. Forgac, The vacuolar (H+)-ATPases—nature's most versatile proton pumps, Nat. Rev. Mol. Cell Biol. 3 (2002) 94–103.
[5] R.H. Fillingame, C.M. Angevine, O.Y. Dmitriev, Mechanics of coupling proton movements to *c*-ring rotation in ATP synthase, FEBS Lett. 555 (2003) 29–34.
[6] M. Futai, G.H. Sun-Wada, Y. Wada, Proton transporting ATPases: introducing unique enzymes coupling catalysis and proton translocation through mechanical rotation, in: M. Futai, Y. Wada, J. Kaplan (Eds.), Handbook of ATPases: Biochemistry, Cell Biology, Pathophysiology, 2004, pp. 237–260.
[7] G.H. Sun-Wada, Y. Wada, M. Futai, Diverse and essential roles of mammalian vacuolar-type proton pump ATPase: toward the physiological understanding of inside acidic compartments, Biochim. Biophys. Acta 1658 (2004) 106–114.
[8] K.W. Beyenbach, H. Wieczorek, The V-type $H^+$ ATPase: molecular structure and function, physiological roles and regulation, J. Exp. Biol. 209 (2006) 577–589.
[9] M. Forgac, Vacuolar ATPases: rotary proton pumps in physiology and pathophysiology, Nat. Rev. Mol. Cell Biol. 8 (2007) 917–929.

[10] V. Marshansky, M. Futai, The V-type $H^+$-ATPase in vesicular trafficking: targeting, regulation and function, Curr. Opin. Cell Biol. 20 (2008) 415–426.
[11] C. von Ballmoos, A. Wiedenmann, P. Dimroth, Essentials for ATP synthesis by $F_1F_0$ ATP synthases, Annu. Rev. Biochem. 78 (2009) 649–672.
[12] J.M. Shin, O. Vagin, K. Munson, G. Sachs, Gastric $H^+$, $K^+$-ATPase, in: M. Futai, Y. Wada, J. Kaplan (Eds.), Handbook of ATPases : Biochemistry, Cell Biology, Pathophysiology, 2004, pp. 179–210.
[13] S. Lecchi, C.W. Slayman, Yeast plasma-membrane $H^+$-ATPase: model system for studies of structure, function, biogenetics, and regulation, in: M. Futai, Y. Wada, J. Kaplan (Eds.), Handbook of ATPases : Biochemistry, Cell Biology, Pathophysiology, 2004, pp. 3–24.
[14] T. Hirata, N. Nakamura, H. Omote, Y. Wada, M. Futai, Regulation and reversibility of vacuolar $H^+$-ATPase, J. Biol. Chem. 275 (2000) 386–389.
[15] M. Nakano, H. Imamura, M. Toei, M. Tamakoshi, M. Yoshida, K. Yokoyama, ATP hydrolysis and synthesis of a rotary motor V-ATPase from *Thermus thermophilus*, J. Biol. Chem. 283 (2008) 20789–20796.
[16] P.D. Boyer, The binding-change mechanism of ATP synthesis, in: C.P. Lee, G. Schatz, L. Ernster (Eds.), Membrane Bioenergetics, Addison-Wesley, Reading, MA, 1979, pp. 461–479.
[17] J.P. Abrahams, A.G. Leslie, R. Lutter, J.E. Walker, Structure at 2.8 Å resolution of $F_1$-ATPase from bovine heart mitochondria, Nature 370 (1994) 621–628.
[18] D. Sabbert, S. Engelbrecht, W. Junge, Intersubunit rotation in active F-ATPase, Nature 381 (1996) 623–625.
[19] T.M. Duncan, V.V. Bulygin, Y. Zhou, M.L. Hutcheon, R.L. Cross, Rotation of subunits during catalysis by *Escherichia coli* $F_1$-ATPase, Proc. Natl. Acad. Sci. USA 92 (1995) 10964–10968.
[20] E.P. Gogol, E. Johnston, R. Aggeler, R.A. Capaldi, Ligand-dependent structural variations in *Escherichia coli* $F_1$ ATPase revealed by cryoelectron microscopy, Proc. Natl. Acad. Sci. USA 87 (1990) 9585–9589.
[21] H. Noji, R. Yasuda, M. Yoshida, K. Kinosita Jr., Direct observation of the rotation of $F_1$-ATPase, Nature 386 (1997) 299–302.
[22] Y. Kato-Yamada, H. Noji, R. Yasuda, K. Kinosita Jr., M. Yoshida, Direct observation of the rotation of epsilon subunit in $F_1$-ATPase, J. Biol. Chem. 273 (1998) 19375–19377.
[23] Y. Sambongi, Y. Iko, M. Tanabe, H. Omote, A. Iwamoto-Kihara, I. Ueda, T. Yanagida, Y. Wada, M. Futai, Mechanical rotation of the *c* subunit oligomer in ATP synthase ($F_0F_1$): direct observation, Science 286 (1999) 1722–1724.
[24] M. Tanabe, K. Nishio, Y. Iko, Y. Sambongi, A. Iwamoto-Kihara, Y. Wada, M. Futai, Rotation of a complex of the γ subunit and *c* ring of *Escherichia coli* ATP synthase. The rotor and stator are interchangeable, J. Biol. Chem. 276 (2001) 15269–15274.
[25] K. Nishio, A. Iwamoto-Kihara, A. Yamamoto, Y. Wada, M. Futai, Subunit rotation of ATP synthase embedded in membranes: α or β subunit rotation relative to the *c* subunit ring, Proc. Natl. Acad. Sci. USA 99 (2002) 13448–13452.
[26] W. Junge, H. Sielaff, S. Engelbrecht, Torque generation and elastic power transmission in the rotary $F_0F_1$-ATPase, Nature 459 (2009) 364–370.
[27] R.K. Nakamoto, J.A. Baylis Scanlon, M.K. Al-Shawi, The rotary mechanism of the ATP synthase, Arch. Biochem. Biophys. 476 (2008) 43–50.
[28] S.D. Watts, Y. Zhang, R.H. Fillingame, R.A. Capaldi, The γ subunit in the *Escherichia coli* ATP synthase complex ($ECF_1F_0$) extends through the stalk and contacts the c subunits of the $F_0$ part, FEBS Lett. 368 (1995) 235–238.
[29] H. Omote, M. Futai, Mutational analysis of $F_1F_0$ ATPase: catalysis and energy coupling, Acta Physiol. Scand. Suppl. 643 (1998) 177–183.
[30] M. Futai, H. Omote, Y. Sambongi, Y. Wada, Synthase ($H^+$ ATPase): coupling between catalysis, mechanical work, and proton translocation, Biochim. Biophys. Acta 1458 (2000) 276–288.
[31] H. Ren, W.S. Allison, On what makes the γ subunit spin during ATP hydrolysis by $F_1$, Biochim. Biophys. Acta 1458 (2000) 221–233.
[32] A.E. Senior, S. Nadanaciva, J. Weber, Rate acceleration of ATP hydrolysis by $F_1F_o$-ATP synthase, J. Exp. Biol. 203 (2000) 35–40.
[33] A.E. Senior, S. Nadanaciva, J. Weber, The molecular mechanism of ATP synthesis by $F_1F_0$-ATP synthase, Biochim. Biophys. Acta 1553 (2002) 188–211.
[34] K. Ida, T. Noumi, M. Maeda, T. Fukui, M. Futai, Catalytic site of $F_1$-ATPase of *Escherichia coli*. Lys-155 and Lys-201 of the β subunit are located near the γ-phosphate group of ATP in the presence of $Mg^{2+}$, J. Biol. Chem. 266 (1991) 5424–5429.
[35] H. Omote, M. Maeda, M. Futai, Effects of mutations of conserved Lys-155 and Thr-156 residues in the phosphate-binding glycine-rich sequence of the $F_1$-ATPase β subunit of *Escherichia coli*, J. Biol. Chem. 267 (1992) 20571–20576.
[36] M.Y. Park, H. Omote, M. Maeda, M. Futai, Conserved Glu-181 and Arg-182 residues of *Escherichia coli* $H^+$-ATPase (ATP synthase) β subunit are essential for catalysis: properties of 33 mutants between βGlu-161 and βLys-201 residues, J. Biochem. 116 (1994) 1139–1145.
[37] S. Löbau, J. Weber, S. Wilke-Mounts, A.E. Senior, $F_1$-ATPase, roles of three catalytic site residues, J. Biol. Chem. 272 (1997) 3648–3656.
[38] S. Nadanaciva, J. Weber, A.E. Senior, The role of β-Arg-182, an essential catalytic site residue in *Escherichia coli* $F_1$-ATPase, Biochemistry 38 (1999) 7670–7677.
[39] A.E. Senior, M.K. Al-Shawi, Further examination of seventeen mutations in *Escherichia coli* $F_1$-ATPase β-subunit, J. Biol. Chem. 267 (1992) 21471–21478.
[40] H. Omote, N.P. Le, M.Y. Park, M. Maeda, M. Futai, β subunit Glu-185 of *Escherichia coli* $H^+$-ATPase (ATP synthase) is an essential residue for cooperative catalysis, J. Biol. Chem. 270 (1995) 25656–25660.
[41] A. Iwamoto, J. Miki, M. Maeda, M. Futai, $H^+$-ATPase γ subunit of *Escherichia coli*. Role of the conserved carboxyl-terminal region, J. Biol. Chem. 265 (1990) 5043–5048.
[42] K. Shin, R.K. Nakamoto, M. Maeda, M. Futai, $F_0F_1$-ATPase γ subunit mutations perturb the coupling between catalysis and transport, J. Biol. Chem. 267 (1992) 20835–20839.
[43] R.K. Nakamoto, M. Maeda, M. Futai, The γ subunit of the *Escherichia coli* ATP synthase. Mutations in the carboxyl-terminal region restore energy coupling to the amino-terminal mutant γMet-23–>Lys, J. Biol. Chem. 268 (1993) 867–872.
[44] R.K. Nakamoto, M.K. Al-Shawi, M. Futai, The ATP synthase γ subunit. Suppressor mutagenesis reveals three helical regions involved in energy coupling, J. Biol. Chem. 270 (1995) 14042–14046.
[45] M.K. Al-Shawi, C.J. Ketchum, R.K. Nakamoto, The *Escherichia coli* $F_0F_1$ γM23K uncoupling mutant has a higher $K_{0.5}$ for $P_i$. Transition state analysis of this mutant and others reveals that synthesis and hydrolysis utilize the same kinetic pathway, Biochemistry 36 (1997) 12961–12969.
[46] C.J. Ketchum, M.K. Al-Shawi, R.K. Nakamoto, Intergenic suppression of the γM23K uncoupling mutation in $F_0F_1$ ATP synthase by βGlu-381 substitutions: the role of the $\beta^{380}$DELSEED$^{386}$ segment in energy coupling, Biochem. J. 330 (Pt 2) (1998) 707–712.
[47] R.N. Lightowlers, S.M. Howitt, L. Hatch, F. Gibson, G.B. Cox, The proton pore in the *Escherichia coli* $F_oF_1$-ATPase: a requirement for arginine at position 210 of the *a* subunit, Biochim. Biophys. Acta 894 (1987) 399–406.
[48] B.D. Cain, R.D. Simoni, Proton translocation by the $F_1F_o$ ATPase of *Escherichia coli*: mutagenic analysis of the α subunit, J. Biol. Chem. 264 (1989) 3292–3300.
[49] S. Eya, M. Maeda, M. Futai, Role of the carboxyl terminal region of $H^+$-ATPase ($F_OF_1$) *a* subunit from *Escherichia coli*, Arch. Biochem. Biophys. 284 (1991) 71–77.
[50] D. Stock, A.G.W. Leslie, J.E. Walker, Molecular architecture of the rotary motor in ATP synthase, Science 286 (1999) 1700–1705.
[51] W. Jiang, J. Hermolin, R.H. Fillingame, The preferred stoichiometry of *c* subunits in the rotary motor sector of *Escherichia coli* ATP synthase is 10, Proc. Natl. Acad. Sci. USA 98 (2001) 4966–4971.
[52] N. Mitome, T. Suzuki, S. Hayashi, M. Yoshida, Thermophilic ATP synthase has a decamer *c*-ring: indication of noninteger 10:3 $H^+$/ATP ratio and permissive elastic coupling, Proc. Natl. Acad. Sci. USA 101 (2004) 12159–12164.
[53] H. Stahlberg, D.J. Muller, K. Suda, D. Fotiadis, A. Engel, T. Meier, U. Matthey, P. Dimroth, Bacterial $Na^+$–ATP synthase has an undecameric rotor, EMBO Rep. 2 (2001) 229–233.
[54] T. Meier, U. Matthey, C. von Ballmoos, J. Vonck, T. Krug von Nidda, W. Kuhlbrandt, P. Dimroth, Evidence for structural integrity in the undecameric *c*-rings isolated from sodium ATP synthases, J. Mol. Biol. 325 (2003) 389–397.
[55] H. Seelert, A. Poetsch, N.A. Dencher, A. Engel, H. Stahlberg, D.J. Muller, Structural biology. Proton-powered turbine of a plant motor, Nature 405 (2000) 418–419.
[56] P. Turina, D. Samoray, P. Gräber, $H^+$/ATP ratio of proton transport-coupled ATP synthesis and hydrolysis catalysed by $CF_0F_1$-liposomes, EMBO J. 22 (2003) 418–426.
[57] D. Pogoryelov, J. Yu, T. Meier, J. Vonck, P. Dimroth, D.J. Muller, The *c*15 ring of the *Spirulina platensis* F-ATP synthase: $F_1/F_0$ symmetry mismatch is not obligatory, EMBO Rep. 6 (2005) 1040–1044.
[58] R.L. Cross, V. Muller, The evolution of A-, F-, and V-type ATP synthases and ATPases: reversals in function and changes in the $H^+$/ATP coupling ratio, FEBS Lett. 576 (2004) 1–4.
[59] L.S. Holliday, M. Lu, B.S. Lee, R.D. Nelson, S. Solivan, L. Zhang, S.L. Gluck, The amino-terminal domain of the B subunit of vacuolar $H^+$-ATPase contains a filamentous actin binding site, J. Biol. Chem. 275 (2000) 32331–32337.
[60] M. Lu, L.S. Holliday, L. Zhang, W.A. Dunn Jr., S.L. Gluck, Interaction between aldolase and vacuolar $H^+$-ATPase: evidence for direct coupling of glycolysis to the ATP-hydrolyzing proton pump, J. Biol. Chem. 276 (2001) 30407–30413.
[61] H. Omote, N. Sambonmatsu, K. Saito, Y. Sambongi, A. Iwamoto-Kihara, T. Yanagida, Y. Wada, M. Futai, The γ-subunit rotation and torque generation in $F_1$-ATPase from wild-type or uncoupled mutant *Escherichia coli*, Proc. Natl. Acad. Sci. USA 96 (1999) 7780–7784.
[62] H. Hosokawa, M. Nakanishi-Matsui, S. Kashiwagi, I. Fujii-Taira, K. Hayashi, A. Iwamoto-Kihara, Y. Wada, M. Futai, ATP-dependent rotation of mutant ATP synthases defective in proton transport, J. Biol. Chem. 280 (2005) 23797–23801.
[63] S.P. Tsunoda, R. Aggeler, M. Yoshida, R.A. Capaldi, Rotation of the *c* subunit oligomer in fully functional $F_1F_O$ ATP synthase, Proc. Natl. Acad. Sci. USA 98 (2001) 898–902.
[64] P.C. Jones, J. Hermolin, R.H. Fillingame, Mutations in single hairpin units of genetically fused subunit *c* provide support for a rotary catalytic mechanism in $F_OF_1$ ATP synthase, J. Biol. Chem. 275 (2000) 11355–11360.
[65] J.A. Scanlon, M.K. Al-Shawi, R.K. Nakamoto, A rotor-stator cross-link in the $F_1$-ATPase blocks the rate-limiting step of rotational catalysis, J. Biol. Chem. 283 (2008) 26228–26240.
[66] M. Diez, B. Zimmermann, M. Börsch, M. König, E. Schweinberger, S. Steigmiller, R. Reuter, S. Felekyan, V. Kudryavtsev, C.A. Seidel, P. Gräber, Proton-powered subunit rotation in single membrane-bound $F_0F_1$-ATP synthase, Nat. Struct. Mol. Biol. 11 (2004) 135–141.
[67] B. Zimmermann, M. Diez, N. Zarrabi, P. Gräber, M. Börsch, Movements of the ε-subunit during catalysis and activation in single membrane-bound $H^+$-ATP synthase, EMBO J. 24 (2005) 2053–2063.
[68] M. Börsch, M. Diez, B. Zimmermann, R. Reuter, P. Gräber, Stepwise rotation of the γ-subunit of $EF_0F_1$-ATP synthase observed by intramolecular single-molecule fluorescence resonance energy transfer, FEBS Lett. 527 (2002) 147–152.
[69] H. Itoh, A. Takahashi, K. Adachi, H. Noji, R. Yasuda, M. Yoshida, K. Kinosita, Mechanically driven ATP synthesis by $F_1$-ATPase, Nature 427 (2004) 465–468.
[70] Y. Rondelez, G. Tresset, T. Nakashima, Y. Kato-Yamada, H. Fujita, S. Takeuchi, H. Noji, Highly coupled ATP synthesis by $F_1$-ATPase single molecules, Nature 433 (2005) 773–777.
[71] R. Yasuda, H. Noji, K. Kinosita Jr., M. Yoshida, $F_1$-ATPase is a highly efficient molecular motor that rotates with discrete 120° steps, Cell 93 (1998) 1117–1124.

[72] K. Adachi, R. Yasuda, H. Noji, H. Itoh, Y. Harada, M. Yoshida, K. Kinosita Jr., Stepping rotation of $F_1$-ATPase visualized through angle-resolved single-fluorophore imaging, Proc. Natl. Acad. Sci. USA 97 (2000) 7243–7247.
[73] R. Yasuda, H. Noji, M. Yoshida, K. Kinosita Jr., H. Itoh, Resolution of distinct rotational substeps by submillisecond kinetic analysis of $F_1$-ATPase, Nature 410 (2001) 898–904.
[74] K. Shimabukuro, R. Yasuda, E. Muneyuki, K.Y. Hara, K. Kinosita Jr., M. Yoshida, Catalysis and rotation of $F_1$ motor: cleavage of ATP at the catalytic site occurs in 1 ms before 40° substep rotation, Proc. Natl. Acad. Sci. USA 100 (2003) 14731–14736.
[75] J.A. Scanlon, M.K. Al-Shawi, N.P. Le, R.K. Nakamoto, Determination of the partial reactions of rotational catalysis in $F_1$-ATPase, Biochemistry 46 (2007) 8785–8797.
[76] S. Nadanaciva, J. Weber, A.E. Senior, New probes of the $F_1$-ATPase catalytic transition state reveal that two of the three catalytic sites can assume a transition state conformation simultaneously, Biochemistry 39 (2000) 9583–9590.
[77] T. Nishizaka, K. Oiwa, H. Noji, S. Kimura, E. Muneyuki, M. Yoshida, K. Kinosita Jr., Chemomechanical coupling in $F_1$-ATPase revealed by simultaneous observation of nucleotide kinetics and rotation, Nat. Struct. Mol. Biol. 11 (2004) 142–148.
[78] K. Adachi, K. Oiwa, T. Nishizaka, S. Furuike, H. Noji, H. Itoh, M. Yoshida, K. Kinosita Jr., Coupling of rotation and catalysis in $F_1$-ATPase revealed by single-molecule imaging and manipulation, Cell 130 (2007) 309–321.
[79] R. Watanabe, R. Iino, K. Shimabukuro, M. Yoshida, H. Noji, Temperature-sensitive reaction intermediate of $F_1$-ATPase, EMBO Rep. 9 (2008) 84–90.
[80] R.I. Menz, J.E. Walker, A.G. Leslie, Structure of bovine mitochondrial $F_1$-ATPase with nucleotide bound to all three catalytic sites: implications for the mechanism of rotary catalysis, Cell 106 (2001) 331–341.
[81] S. Furuike, K. Adachi, N. Sakaki, R. Shimo-Kon, H. Itoh, E. Muneyuki, M. Yoshida, K. Kinosita Jr., Temperature dependence of the rotation and hydrolysis activities of $F_1$-ATPase, Biophys. J. 95 (2008) 761–770.
[82] M. Nakanishi-Matsui, S. Kashiwagi, H. Hosokawa, D.J. Cipriano, S.D. Dunn, Y. Wada, M. Futai, Stochastic high-speed rotation of *Escherichia coli* ATP synthase $F_1$ sector: the ε subunit-sensitive rotation, J. Biol. Chem. 281 (2006) 4126–4131.
[83] M. Nakanishi-Matsui, S. Kashiwagi, T. Ubukata, A. Iwamoto-Kihara, Y. Wada, M. Futai, Rotational catalysis of *Escherichia coli* ATP synthase $F_1$ sector. Stochastic fluctuation and a key domain of the β subunit, J. Biol. Chem. 282 (2007) 20698–20704.
[84] M. Nakanishi-Matsui, M. Futai, Stochastic proton pumping ATPases: from single molecules to diverse physiological roles, IUBMB Life 58 (2006) 318–322.
[85] M. Nakanishi-Matsui, M. Futai, Stochastic rotational catalysis of proton pumping F-ATPase, Philos. Trans. R. Soc. Lond. B Biol. Sci. 363 (2008) 2135–2142.
[86] M. Sekiya, R.K. Nakamoto, M.K. Al-Shawi, M. Nakanishi-Matsui, M. Futai, Temperature dependence of single molecule rotation of the *Escherichia coli* ATP synthase $F_1$ sector reveals the importance of γ–β subunit interactions in the catalytic dwell, J. Biol. Chem. 284 (2009) 22401–22410.
[87] H. Yagi, N. Kajiwara, T. Iwabuchi, K. Izumi, M. Yoshida, H. Akutsu, Stepwise propagation of the ATP-induced conformational change of the $F_1$-ATPase β subunit revealed by NMR, J. Biol. Chem. 284 (2009) 2374–2382.
[88] A. Iwamoto, H. Omote, H. Hanada, N. Tomioka, A. Itai, M. Maeda, M. Futai, Mutations in Ser174 and the glycine-rich sequence (Gly149, Gly150, and Thr156) in the β subunit of *Escherichia coli* $H^+$-ATPase, J. Biol. Chem. 266 (1991) 16350–16355.
[89] S. Kashiwagi, A. Iwamoto-Kihara, M. Kojima, T. Nonaka, M. Futai, M. Nakanishi-Matsui, Effects of mutations in the β subunit hinge domain on ATP synthase $F_1$ sector rotation: interaction between Ser 174 and Ile 163, Biochem. Biophys. Res. Commun. 365 (2008) 227–231.
[90] H. Kanazawa, H. Hama, B.P. Rosen, M. Futai, Deletion of seven amino acid residues from the γ subunit of *Escherichia coli* $H^+$-ATPase causes total loss of $F_1$ assembly on membranes, Arch. Biochem. Biophys. 241 (1985) 364–370.
[91] M.K. Al-Shawi, R.K. Nakamoto, Mechanism of energy coupling in the $F_OF_1$-ATP synthase: the uncoupling mutation, γM23K, disrupts the use of binding energy to drive catalysis, Biochemistry 36 (1997) 12954–12960.
[92] M.K. Al-Shawi, C.J. Ketchum, R.K. Nakamoto, Energy coupling, turnover, and stability of the $F_OF_1$ ATP synthase are dependent on the energy of interaction between γ and β subunits, J. Biol. Chem. 272 (1997) 2300–2306.
[93] T. Hirata, A. Iwamoto-Kihara, G.H. Sun-Wada, T. Okajima, Y. Wada, M. Futai, Subunit rotation of vacuolar-type proton pumping ATPase: relative rotation of the G and C subunits, J. Biol. Chem. 278 (2003) 23714–23719.
[94] H. Imamura, M. Nakano, H. Noji, E. Muneyuki, S. Ohkuma, M. Yoshida, K. Yokoyama, Evidence for rotation of $V_1$-ATPase, Proc. Natl. Acad. Sci. USA 100 (2003) 2312–2315.
[95] K. Yokoyama, M. Nakano, H. Imamura, M. Yoshida, M. Tamakoshi, Rotation of the proteolipid ring in the V-ATPase, J. Biol. Chem. 278 (2003) 24255–24258.
[96] H. Imamura, M. Takeda, S. Funamoto, K. Shimabukuro, M. Yoshida, K. Yokoyama, Rotation scheme of $V_1$-motor is different from that of $F_1$-motor, Proc. Natl. Acad. Sci. USA 102 (2005) 17929–17933.
[97] T. Meier, P. Polzer, K. Diederichs, W. Welte, P. Dimroth, Structure of the rotor ring of F-type $Na^+$-ATPase from *Ilyobacter tartaricus*, Science 308 (2005) 659–662.
[98] K. Hayashi, G.H. Sun-Wada, Y. Wada, M. Nakanishi-Matsui, M. Futai, Defective assembly of a hybrid vacuolar $H^+$-ATPase containing the mouse testis-specific *E*1 isoform and yeast subunits, Biochim. Biophys. Acta 1777 (2008) 1370–1377.
[99] M.W. Bowler, M.G. Montgomery, A.G. Leslie, J.E. Walker, Ground state structure of $F_1$-ATPase from bovine heart mitochondria at 1.9 Å resolution, J. Biol. Chem. 282 (2007) 14238–14242.